Self-Assembly of Square Molecular Boxes Containing Dirhodium(II,II) Units

Sandra Lo Schiavo,*[a] Gabriella Pocsfalvi,[b] Scolastica Serroni,[a] Paola Cardiano,[a] and Pasquale Piraino*[a]

Keywords: Macrocycles / Dirhodium compounds / Porphyrins / Mass spectrometry

Dirhodium(II,II) based square molecular boxes were easily obtained by reaction of $[Rh_2(form)_2(CF_3COO)_2(H_2O)_2]$ (form = *N*,*N*′-di-*p*-tolylformamidinate) with both linear (terephthalate and oxalate) and angular [5,10-diphenyl-15,20-bis(4-carboxyphenyl)porphyrin] dicarboxylate dianions; liquid secondary ionization mass spectrometry (LSI MS) was used to establish the nuclearity of the new macrocycles. Their electrochemical properties were also investigated.

Introduction

Self-assembly of so-called "molecular squares" by means of appropriate transition metal complexes represents an attractive field of current research owing to their implication in nanotechnology. The molecular squares so far reported are mainly based on *cis*-coordinated square-planar transition metal complexes and rigid or semirigid bidentate ligands as connectors or, alternatively, on *trans* square-planar metal complexes as connectors and bidentate angular units.[1] In any case this synthetic strategy, which requires transition metal complexes with two *cis*- or *trans*-coordinated labile ligands, has been limited to the use of mononuclear transition metal complexes as building blocks.[1] Only recently have molecular squares incorporating dinuclear species as corner units have been reported.[2]

Our experience in the chemistry of dirhodium(II,II) complexes with "lantern" structures led us to plan the synthesis of molecular boxes involving dirhodium(II,II) species. These complexes, in addition to the well-known redox and axial reactivity, may exhibit equatorial reactivity too. In fact, the complex $[Rh_2(form)_2(CF_3COO)_2(H_2O)_2]$ (**1**) (form = *N*,*N*′-di-*p*-tolylformamidinate), characterized by two formamidinate and two trifluoroacetate groups symmetrically bridged in a cisoid arrangement around the Rh_2^{4+} core, exhibits a remarkable lability of the trifluoroacetate groups.[3] This leads to mild conditions for the substitution of neutral bidentate ligands at the equatorial positions without rupture of the cisoid $Rh_2(form)_2$ fragment.[4] Furthermore, complex **1** has been successfully used to synthesize a series of new mixed dirhodium(II,II) derivatives by metathetical reactions with a variety of carboxylates.[5]

These results show that **1** may be able to act as an appropriate precursor of angular building blocks, through the *cis*-$Rh_2(form)_2$ fragment, which is able to produce neutral square molecular boxes in combination with the appropriate dicarboxylate dianions as ligand connectors. The nuclearity of the boxes will depend on the dicarboxylates used: linear dicarboxylates will generate boxes with four $Rh_2(form)_2$ units at the corners, while angular ones will generate boxes with two alternating $Rh_2(form)_2$ units at the corners.

This paper deals with the synthesis and LSI MS (Liquid Secondary Ionization Mass Spectrometry) characterization of the square molecular boxes $[Rh_2(form)_2(tp)]_4$ (tp = terephthalate) (**2**), $[Rh_2(form)_2(ox)]_4$ (ox = oxalate) (**3**) and $[Rh_2(form)_2(porphy\{COO\}_2)]_2$ (**4**) [porphy$(COO)_2$] = 15,20-di-(4-carboxyphenyl)-5,10-diphenylporphyrin] incorporating the $Rh_2(form)_2$ fragment as angular units. These macrocycles represent the first examples of square molecular boxes incorporating dirhodium units as building blocks; while the manuscript was in preparation Cotton et al. anticipated the synthesis of **3**.[2]

More interestingly, looking at the redox properties of porphyrins [porphy$(COO)_2$, E = +1.1 V vs. SCE in 1,2-dichloroethane] and $[Rh_2(form)_2(CF_3COO)_2(H_2O)_2]$ [$E°(Rh_2^{4+}/Rh_2^{5+})$ = +0.59 V vs. SCE in CH_2Cl_2], **2**, **3** and **4** represent examples of multiredox molecular squares. The paper also reports a study of their redox behaviour as well as the luminescence properties of **4**.

Results and Discussion

Synthesis and Characterization

$[Rh_2(form)_2(dicarboxylate)]_4$: Treatment of $[Rh_2(form)_2(CF_3COO)_2(H_2O)_2]$ with an excess of terephthalate (tp) or oxalate (ox) disodium salts results in the formation of $[Rh_2(form)_2(tp)]_4$ (**2**) or $[Rh_2(form)_2(ox)]_4$ (**3**) in good yields. Both the compounds are green stable solids, which we were unable to obtain in a suitable crystalline form. Their solution behaviour and their spectroscopic features closely resemble those of the parent dinuclear species, **1**.[3] IR and proton NMR spectroscopic data unambiguously show that the formamidinate and carboxylate groups are coordinated

[a] Dipartimento di Chimica Inorganica, Chimica Analitica e Chimica Fisica, Università di Messina,
Salita Sperone n. 31, 98166 Vil. S. Agata, Messina, Italy
E-mail: loschiavo@chem.unime.it
[b] Centro Internazionale di Servizi di Spettrometria di Massa del C.N.R.,
Via P. Castellino 111−80131 Napoli, Italy

  1434−1948/00/0606−1371 $ 17.50+.50/0

in the usual way, namely symmetrically bridged across the Rh_2^{4+} core. The proposed structures for **2** and **3** (Figure 1) were determined by elemental analysis and LSI MS spectrometry. Mass spectrometry using different "soft" ionisation techniques, namely LSI, ESI (electrospray ionisation) and MALDI (matrix assisted laser desorption) is currently used, in the absence of X-ray data, as a powerful tool for establishing the structure of compounds of this type.[1,6]

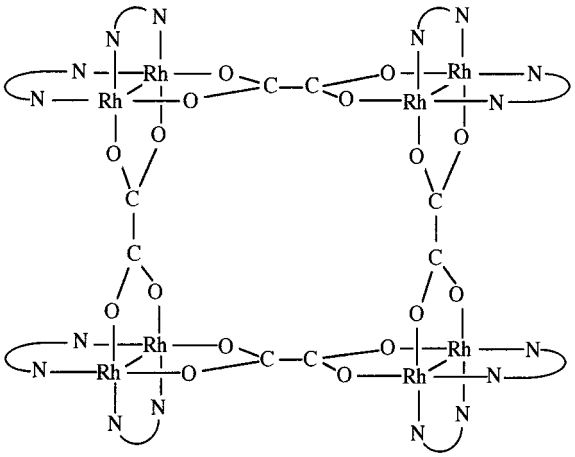

Figure 1. Proposed structure for $[Rh_2(form)_2(ox)]_4$ (**3**)

The positive ion LSI mass spectrum of **2** yields an abundant protonated molecular ion (MH^+) peak at *m/z* = 3265.5 (the *m/z* values reported here are the measured isotopically resolved, ^{12}C-containing, monoisotopic mass-to-charge ratios) corresponding to the expected $[Rh_2(form)_2(tp)]_4H^+$ composition. The loss of one or two hydrogen atoms from MH^+ can be observed with relative abundances of 50 and 15 percent to the monoisotopic molecular ion peak, respectively. This was to be found characteristic of all the three compounds investigated here. The loss of hydrogen is a frequently observed fragmentation process for molecules under conditions of liquid secondary ionization. This determines a difference in the appearance of the isotope peak cluster with respect to that theoretically expected.[7] The spectrum also shows less abundant peaks, with $[Rh_2(form)_2(tp)]_3H^+$ and $[Rh_2(form)_2(tp)]_2H^+$ compositions, at *m/z* = 2449.5 and 1633.3, respectively, which could be indicative of a systematic fragmentation of the molecule upon ionization, or, in the light of recent reports, of the presence of by-products in the sample.[2]

The LSI MS spectrum of **3** results in a base peak at *m/z* = 2961.3 (MH^+), with an isotopic distribution consistent with the expected protonated molecular ion with hydrogen loss. In this case a probe-accurate mass measurement on the MH^+ peak cluster was performed. The exact mass of the monoisotopic molecular ion peak was measured to be 2961.1581 (theoretically calculated mass is 2961.1587 for $C_{128}H_{121}N_{16}O_{16}Rh_8$ with an error of 0.2 ppm) again giving evidence for hydrogen loss. A doubly charged molecular ion (MH_2^{2+}) is also found at *m/z* = 1482.7. Analogously to the spectrum of **2**, peaks with lower abundance, corresponding to $[Rh_2(form)_2(ox)]_2H^+$ and $[Rh_2(form)_2(ox)]_3H^+$, are observed at *m/z* = 1481.2 and 2221.0, respectively.

$[Rh_2(form)_2(dicarboxylate)]_2$: We also turned our attention to self-assembly of the $Rh_2(form)_2$ fragments with functionalized porphyrins which, in the past, have been successfully used both as linear and angular connectors.[8,9] In particular we planned the synthesis of molecular boxes of lower nuclearity by combining two angular building units such as $[Rh_2(form)_2]$ and 15,20-di-(4-carboxyphenyl)-5,10-diphenylporphyrin.

$[Rh_2(form)_2(CF_3COO)_2(H_2O)_2]$ reacts with the disodium salt of 15,20-di-(4-carboxyphenyl)-5,10-diphenylporphyrin affording the complex $[Rh_2(form)_2(porphy\{COO\}_2)]_2$ (**4**) (Figure 2).

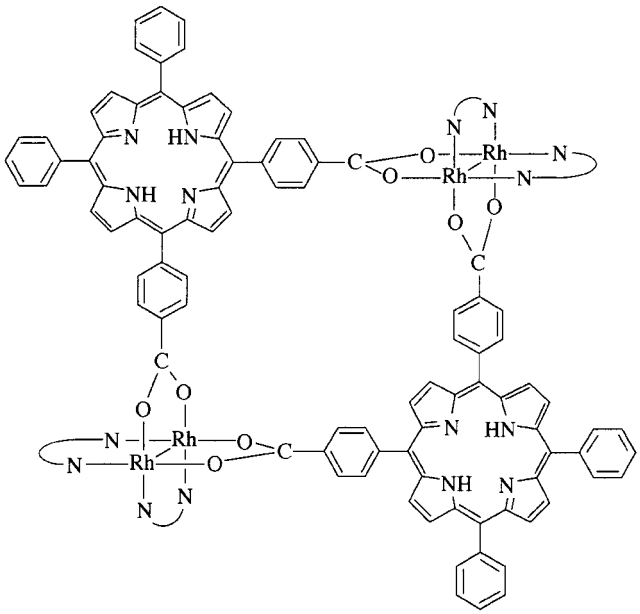

Figure 2. Proposed structure for $[Rh_2(form)_2(porphy\{COO\}_2)]_2$ (**4**)

Compound **4** is a dark red-brown microcrystalline solid very soluble in benzene and chlorinated solvents and sparingly soluble in coordinating solvents. ^1H NMR and IR spectroscopic data were consistent with the proposed structure. Even in this case LSI MS mass spectrometry was employed to assess the nuclearity of **4** (Figure 3). The mass spectrum yields the molecular ion peak (MH^+) at *m/z* = 2705.7, with a good isotopic resolution, as shown in Figure 3. No other significant peak is noted in the spectrum. The slight difference in the measured isotopic distribution with respect to the theoretical pattern of MH^+ rises from the loss of one or two hydrogen atoms from MH^+, as already observed in the mass spectra of **2** and **3**.[7]

Electrochemistry

The electrochemical data for this new family of molecular squares are collected in Table 1, together with those of the parent complex **1**, $[Rh_2(form)_4]$ and the uncoordinated porphy$(COO)_2$ ligand. The cyclic voltammograms of all the compounds are shown in Figure 4.

As shown in Figure 4a, the macrocycle **3** undergoes three reversible oxidations. A cursory look at the data reported

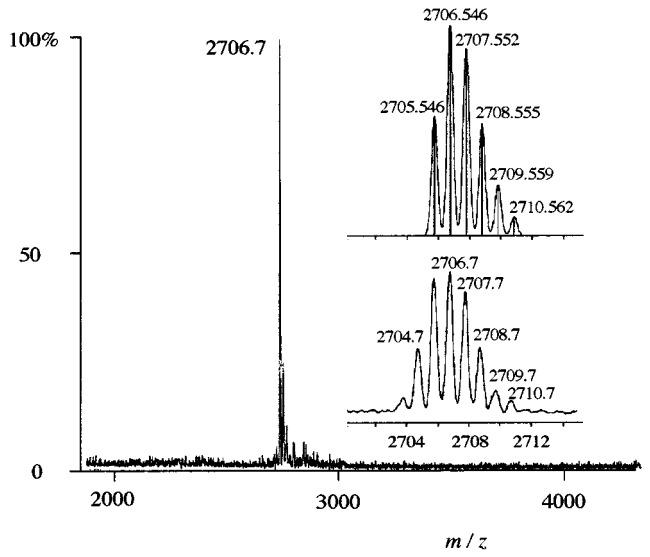

Figure 3. LSI mass spectrum of **4**, including the calculated (top) and experimental (bottom) isotopic distribution of MH^+

Table 1. Redox data; experiments were performed in argon-purged 1,2-dichloroethane solutions; all the processes are reversible except where otherwise noted; the number of exchanged electrons are reported in brackets

Compound	Oxidation (V vs. SCE)[a]		Reduction (V vs. SCE[a])
3	+0.42,[2] +0.57[2]	+1.41[4]	
2	+ 0.43[4]	+1.30[4]	
4	+0.38,[2] +1.11[b]	+1.37[b]	−1.12[2]
1[c]	+0.59[1]	+1.40[1]	
$[Rh_2(form)_4]$[c]	+0.12	+0.95	
$Porphy(COO)_2$[d]	+1.10[b]		−1.18[b]

[a] $E_{1/2}$ values are reported for reversible processes and E_{peak} values are reported for irreversible processes. − [b] Irreversible process. − [c] Data obtained in dichloromethane solution. The two one-electron reversible oxidations of **1** and $[Rh_2(form)_4]$ are due to Rh_2^{4+}/Rh_2^{5+} and Rh_2^{5+}/Rh_2^{6+} processes, respectively.[10] − [d] The oxidation and reduction processes of the uncoordinated porphyrin are centered in the π and π* molecular orbitals of the porphyrin framework, respectively.

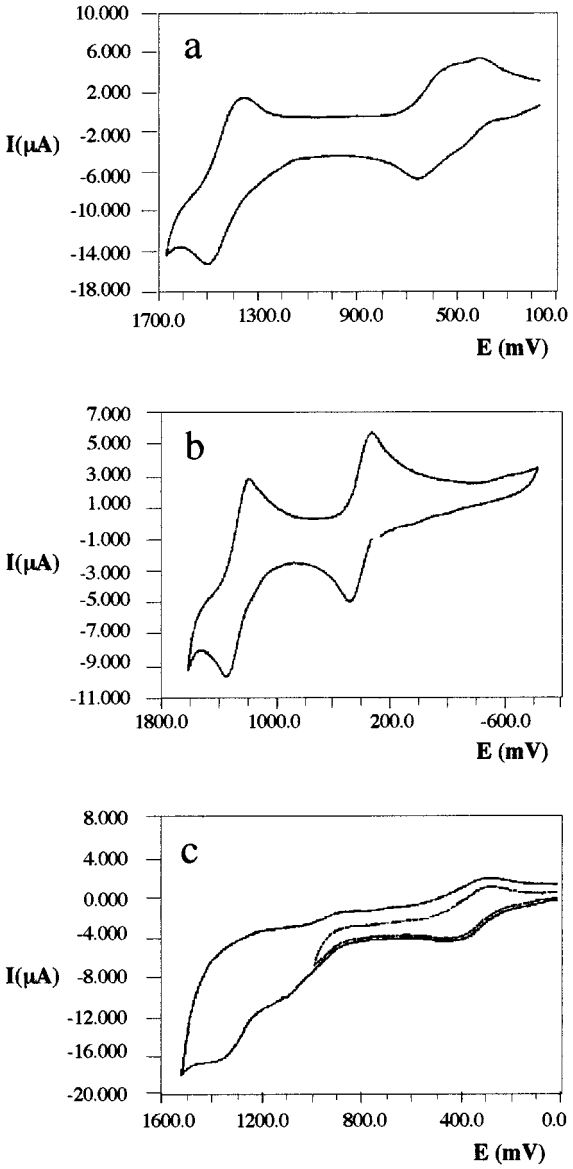

Figure 4. Cyclic voltammograms of **3** (a), **2** (b), and **4** (c); for **4** the CV obtained by scanning the potential up to +1 vs. SCE is also shown to underline the increase of the reversibility of the first process in the absence of the second and third oxidations

in Table 1 allows us to assign the first two anodic processes to the Rh_2^{4+}/Rh_2^{5+} oxidation and the third one to Rh_2^{5+}/Rh_2^{6+}. It is interesting to note that the two bielectronic Rh_2^{4+}/Rh_2^{5+} oxidation processes occur at very close potential values. These anodic processes are shifted to lower potentials with respect to that of **1** and significantly higher with respect to that of $[Rh_2(form)_4]$ as a consequence of the different electron richness of the complexes.[10] Most likely, the first dirhodium units to be oxidized are at opposite corners of the box, with no electronic interaction between them: therefore, the process at +0.42 V is best described as a two simultaneous one-electron process involving noninteracting units.[11] The CV response of **4** (Figure 4c), which does not show splitting of the Rh_2^{4+}/Rh_2^{5+} oxidation processes, supports this suggestion. The following oxidation (+0.57 V) may be assigned to two simultaneous one-electron processes involving the unoxidized Rh_2^{4+} units, whose value is displaced to more positive potential because of the interactions with the nearby Rh_2^{5+} corners. The third oxidation (+1.41 V) can be assigned to four simultaneous one-electron processes involving all the Rh_2^{5+} units and leading to Rh_2^{6+} species. This oxidation pattern suggests that the electronic interaction among Rh_2^{4+} units in the molecular square is larger than that among the Rh_2^{5+} ones.

The CV pattern of **2** (see Figure 4b) resembles that of the parent complex **1** and $[Rh_2(form)_4]$ and is significantly different from **3**. The CV and DPV experiments indicate two quantitatively identical processes, arising from two successive series of four simultaneous one-electron oxidations leading to Rh_2^{5+} and Rh_2^{6+} species, respectively. The decreased interaction between the Rh_2^{4+} units in **2** with respect to **3**, evidenced by the absence of the splitting of the Rh_2^{4+}/Rh_2^{5+} processes, reflects the larger distance between the dirhodium units.

On the basis of the assignment of the CV response given by **2** and **3** and porhy$(COO)_2$, the redox behaviour of **4** appears straightforward (Figure 4c). The first oxidation is reasonably assigned to two simultaneous Rh_2^{4+}/Rh_2^{5+} processes, the second one to the oxidation of both porphyrins, and the third one to the simultaneous Rh_2^{5+}/Rh_2^{6+} oxidation processes of the Rh_2 cores. Although a precise estimation of the exchanged electrons cannot be obtained for the second and third oxidations because of their irreversible nature, an analysis of the intensity of the cathodic peaks suggests that these processes also involve two electrons each. The irreversibility of the Rh_2^{5+}/Rh_2^{6+} process in **4** is probably a consequence of the irreversible porphyrin-based oxidation which precedes such a process. The reduction process of **4** is easily assigned as a porphyrin-based process, on the basis of the reduction behaviour of the uncoordinated porphyrin (Table 1).

Luminescence

Complexes **1**, **2**, and **3** are not emissive in fluid solution at room temperature. On the contrary, however, compound **4** exhibits a room-temperature emission with maxima at $\lambda = 648$ nm and $\lambda = 712$ nm, assigned to the porphyrin units.[12] Interestingly, such an emission is strongly reduced ($\Phi = 7 \times 10^{-5}$; $\tau < 500$ ps, which is the limit of our apparatus) with respect to the free porphyrin emission ($\Phi = 0.017$; $\tau = 10$ ns), although it is spectrally identical. The luminescence decrease can most likely be attributed to reductive electron-transfer quenching of the porphyrin excited state by the dirhodium units. This process is indeed exoergonic, by about 0.4 eV, on the basis of redox and photophysical data.[13] The rate constant of the process, calculated by taking into account the luminescence quantum yields of **4** and the free porphyrin, and the luminescence lifetime of the free porphyrin, is of the order of 10^{11} s^{-1}, in agreement with literature data concerning electron transfer at relatively short distances.[14]

Conclusions

As a final comment we would like to underline that dirhodium(II,II) compounds appear to be suitable substrates for the construction of molecular squares and, by exploiting their well-known axial reactivity, to connect these to form square channels.

Furthermore, besides providing angular building blocks, they may also be used as *exo*-bidentate building blocks linking angular species through their two axial coordination sites. This synthetic strategy opens the way to the construction of a large variety of dirhodium(II,II) based molecular boxes simply varying the angular connectors.

Experimental Section

Materials: The starting complex $[Rh_2(form)_2(CF_3COO)_2(H_2O)_2]$ was prepared according to a published procedure.[3] The 15,20-di-(4-carboxyphenyl)-5,10-diphenylporphyrin was purchased from Mid-Century Company, Illinois. All other chemicals are commercially available and were used as supplied. None of the compounds reported here are air sensitive, but all reactions were carried out under an atmosphere of dry nitrogen. Elemental analyses were performed by REDOX snc Laboratorio di Microanalisi, Cologno Monzese (Milano), Italy.

Apparatus: Infrared spectra were recorded as KBr pellets with a Perkin−Elmer FT 1720X spectrometer. Electronic absorption spectra were recorded on a Perkin−Elmer Lambda 5 UV/Visible spectrophotometer. The NMR measurements were performed with a Bruker AMX 300 spectrometer using standard pulse sequences. Liquid secondary ion mass spectrometry (LSI MS) experiments were carried out on a VG-ZAB-T (Micromass, Wythenshawe, Manchester, U.K.) four-sector mass spectrometer equipped with a 40 kV caesium ion gun. Ionization was achieved by bombardment of 30 keV of caesium ions. Samples were dissolved in chloroform. Mass spectra were obtained employing 1μL of *m*NBA matrix followed by careful addition of 1 μL sample solution on the probe. The spectra were recorded in the positive ion mode at 8 kV accelerating potential. The resolution was set to 2500 (static resolution measured at 5% valley definition), mass range was $m/z = 1500-4200$ with a scan rate 8 s $decade^{-1}$. Ions were detected by a photomultiplier detector and acquisitions were performed in continuum mode using the OPUS V3.1X software. Calibration of the mass scale was carried out on the cluster peaks of CsI. The average error was measured to be less than 0.2 Da for the entire mass range. Probe-accurate mass measurement was performed using a slow linear voltage scanning at 8000 resolution and applying polyethylene glycol as internal calibrant.

Electrochemical measurements were carried out in argon-purged 1,2-dichloroethane at room temperature with a PAR 273 multipurpose equipment interfaced to a PC. The working electrode was a glassy carbon (8 mm^2, Amel) electrode. The counter electrode was a Pt wire, and the quasi-reference electrode was an Ag wire (ferrocene was used as internal standard). The concentration of the complexes was about 5×10^{-4} M. Tetrabutylammonium hexafluorophosphate was used as supporting electrolyte and its concentration was 0.05 M. Cyclic voltammograms were obtained at scan rates of 20, 50, 200, and 500 mV/s. For reversible processes, half-wave potentials (vs. SCE) were calculated as the average of the cathodic and anodic peaks. The criteria for reversibility were the separation between cathodic and anodic peaks, the close to unity ratio of the intensities of the cathodic and anodic currents, and the constancy of the peak potential on changing scan rate. For irreversible processes, the values reported in Table 1 are the peaks estimated by differential pulse voltammetry (DPV). The number of exchanged electrons was measured with differential pulse voltammetry (DPV) experiments performed with a scan rate of 20 mV/s, a pulse height of 75 mV, and a duration of 40 ms. Experimental error on the redox potentials is ± 10 mV.

The luminescence experiments were performed in air-equilibrated dichloromethane solution at 298 K. Luminescence spectra have been obtained with a Jobin Yvon-Spex Fluoromax 2 fluorimeter. The spectra were corrected for detector response. Luminescence lifetimes were measured with an Edinburgh FL 900 time-correlated single-photon-counting spectrometer, with nitrogen discharge as the excitation pulse and using a Marquadt algorithm for pulse deconvolution. Luminescence quantum yields have been calculated by the optically diluted method,[15] using $Ru(bpy)_3^{2+}$ as quantum yield standard ($\Phi = 0.028$) in air-equilibrated aqueous solution.[16]

Experimental uncertainties on luminescence spectra, lifetimes and quantum yields are ± 2 nm, 10%, and 20%, respectively.

Syntheses

$[Rh_2(form)_2(tp)]_4$ (2): To an aqueous solution (40 mL) of disodium terephthalate (0.300 g, 1.43 mmol) was added a chloroform/acetone solution (1:3, 20 mL) of **1** (0.200 mg, 0.218 mol) and the resulting mixture left to stir for ca. 24 h. After this time the organic volatiles were removed on a rotary evaporator and the green solid was collected by filtration, washed several times with warm water and methanol and dried. The crude green solid was then dissolved in $CHCl_3$ (30 mL) and filtered through Celite. Addition of *n*-hexane (20 mL) to the filtrate afforded **2** (0.156 g, 0.048 mmol) as a green precipitate in 88% yield. − $C_{38}H_{34}N_4O_4Rh_2$: calcd. C 55.9, H 4.20, N 6.86; found C 55.64, H 4.30, N 6.88. − IR (KBr): $\nu_{asym}(CO_2)$ = 1620 (s), ν(N−C−N) = 1591 cm^{-1} (s). − UV/Vis ($CHCl_3$): λ_{max} = 520, 630. − LSI MS: *m/z* (%) = 3265.5 (100) [MH^+], 2449.5 (10) [$\{Rh_2(form)_2(tp)\}_3H^+$], 1633.3 (10) [$\{Rh_2(form)_2(tp)\}_2H^+$].

$[Rh_2(form)_2(ox)]_4$ (3): Complex **3** was prepared by following the same procedure as used for **2**. Yield 80%. − $C_{32}H_{30}N_4O_4Rh_2$: calcd. C 51.91, H 4.08, N 7.57; found C 51.95, H 4.44, N 7.26. − IR (KBr): $\nu_{asym}(CO_2)$ = 1626 (s), ν(N−C−N)= 1598 cm^{-1} (s). − UV/Vis ($CHCl_3$): λ_{max} = 625. − ^1H NMR ($CDCl_3$): δ = 2.23 (s, 12 H, CH_3), 6.80 (dd, *J* = 19.4 and 7.9 Hz, 16 H, H_{tol}), 7.41 (t, br, 2 H, N−CH−N). − LSI MS: *m/z* (%) = 2961.2 (100) [MH^+], 1482.7 [MH_2^{2+}], 2221.0 (5) [$\{Rh_2(form)_2(ox)\}_3H^+$], 1481.2 (5) [$\{Rh_2(form)_2(ox)\}_2H^+$].

$[Rh_2(form)_2(porphy\{COO\}_2)]_2$ (4): To a methanol (20 mL) mixture of 15,20-di-(4-carboxyphenyl)-5,10-diphenylporphyrin (0.120 g, 0.171 mmol) was added an aqueous solution (10 mL) of NaOH (0.015 g, 0.375 mmol). The resulting solution was stirred for ca. 30 min and then filtered. A chloroform solution (10 mL) of **1** (0.110 g, 0.121 mmol) was added dropwise to the filtrate and the resulting mixture left to stir for 24 h. During this time **4** was formed as a dark red-brown solid, which was collected by filtration and crystallized from benzene/*n*-heptane. Yield 55%. − $C_{76}H_{58}N_8O_4Rh_2$: calcd. C 67.96, H 4.32, N 8.28; found C 66.21, H 4.58, N 8.48. − IR (KBr): $\nu_{asym}(CO_2)$ = 1620 (m), ν(N−C−N) = 1594 cm^{-1} (s). − UV/Vis ($CHCl_3$): λ_{max} = 419, 515, 549, 589, 644 nm. − ^1H NMR ($CDCl_3$): δ = −2.85 (s, 2 H), 2.23 (s, 12 H), 7.11 (m, 16 H), 7.79 (m, 10 H), 8.23 (m, 8 H), 8.55 (t, br, 2 H), 8.88 (s, 8 H). − LSI MS: *m/z* (%) = 2705.9 (100) [MH^+].

Acknowledgments

We thank the Italian CNR and the MURST for financial support.

[1] M. Fujita, J. Yazaki, K. Ogura, *J. Am. Chem. Soc.* **1990**, *112*, 5645−5647; P. J. Stang, D. H. Cao, *J. Am. Chem. Soc.* **1994**, *116*, 4981−4982; P. J. Stang, D. H. Cao, S. Saito, *J. Am. Chem. Soc.* **1995**, *117*, 6273−6283; P. J. Stang, D. H. Cao, K. Chen, M. Gray, D. C. Muddiman, R. D. Smith, *J. Am. Chem. Soc.* **1997**, *119*, 5163−5168; P. J. Stang, K. Chen, *J. Am. Chem. Soc.* **1995**, *117*, 1667−1668; P. J. Stang, K. Chen, M. Arif, *J. Am. Chem. Soc.* **1995**, *117*, 8793−8797; C. Muller, J. A. Whiteford, P. J. Stang, *J. Am. Chem. Soc.* **1998**, *120*, 9827. Recent review references: B. Olenyuk, A. Fechtenkotter, P. J. Stang, *J. Chem. Soc., Dalton Trans.* **1998**, 1707−1729; M. Fujita, *Chem. Soc. Rev.* **1998**, 417−425.

[2] F. A. Cotton, L. M. Daniels, C. Lin, C. A. Murrillo, *J. Am. Chem. Soc.* **1999**, *121*, 4538−4539; J. L. Heinrich, P. A. Berseth, J. R. Long, *Chem. Commun.* **1998**, 1231−1232; P. Thuéry, M. Nierlich, B. W. Baldwin, N. Komatsuzaki, T. Hirose, *J. Chem. Soc., Dalton Trans.* **1999**, 1047−1048; H. Rauter, I. Mutikainen, M. Blomberg, C. J. L. Lock, P. Amo-Ochoa, E. Freisinger, L. Randaccio, E. Zangrando, E. Chiarparin, B. Lippert, *Angew. Chem. Int. Ed. Engl.* **1997**, *36*, 1296−1301.

[3] P. Piraino, G. Bruno, G. Tresoldi, S. Lo Schiavo, P. Zanello, *Inorg. Chem.* **1987**, *26*, 91−96.

[4] P. Piraino, G. Bruno, S. Lo Schiavo, F. Laschi, P. Zanello, *Inorg. Chem.* **1987**, *26*, 2205−2211; G. A. Rizzi, M. Casarin, E. Tondello, P. Piraino, G. Granozzi, *Inorg. Chem.* **1987**, *26*, 3406−3409; E. Rotondo, B. E. Mann, P. Piraino, G. Tresoldi, *Inorg. Chem.* **1989**, *28*, 3070−3073; E. Rotondo, G. Bruno, F. Nicolò, S. Lo Schiavo, P. Piraino, *Inorg. Chem.* **1991**, *30*, 1195−1200; P. Piraino, G. Tresoldi, S. Lo Schiavo, *Inorg. Chim. Acta.* **1993**, *203*, 101−105; G. Bruno, G. De Munno, G. Tresoldi, S. Lo Schiavo, P. Piraino, *Inorg. Chem.* **1992**, *31*, 1538−1540; S. Lo Schiavo, M. S. Sinicropi, G. Tresoldi, C. G. Arena, P. Piraino, *J. Chem. Soc., Dalton Trans.* **1994**, 1517−1522; G. Tresoldi, G. De Munno, F. Nicolò, S. Lo Schiavo, P. Piraino, *Inorg. Chem.* **1996**, *35*, 1377−1381.

[5] S. Lo Schiavo et al., manuscript in preparation.

[6] T. G. Schaaff, Y. Qu, N. Farrell, V. H. Wysocki, *J. Mass Spectrom.* **1998**, *33*, 436−443; J. Manna, C. J. Kuehl, J. A. Whiteford, P. J. Stang, D. C. Muddiman, S. A. Hofstadler, R. D. Smith, *J. Am.Chem. Soc.* **1997**, *119*, 11611−11619.

[7] K. Vekey, *Int. J. Mass Spectrom. Ion Proc.* **1990**, *97*, 265−282; K. Vekey, L. F. Zerilli, *Org. Mass Spectrom.* **1991**, *26*, 939−944.

[8] C. M. Drain, J.-M. Lehn, *J. Chem. Soc., Chem. Commun.* **1994**, 2313−2315.

[9] P. J. Stang, J. Fan, B. Olenyuk, *Chem. Commun.* **1997**, 1453−1454.

[10] S. Lo Schiavo, G. Bruno, P. Zanello, F. Laschi, P. Piraino, *Inorg. Chem.* **1997**, *36*, 1004−1012.

[11] J. B. Flanagan, S. Margel, A. J. Bard, F. C. Anson, *J. Am. Chem. Soc.* **1978**, *100*, 4248−4253.

[12] K. Kalyanasundaram, *Photochemistry of Polypyridine and Porphyrin Complexes*, Academic Press, London, UK, **1992**.

[13] The driving force Δ*E* for the reductive electron-transfer quenching has been calculated by applying the equation $\Delta E = e(E_{ox} - {}^*E_{red})$, where work terms and entropy contributions are neglected. E_{ox} is the oxidation potential of the dirhodium subunits and $^*E_{red}$ is the excited-state reduction potential of the porphyrin units in **4**. In turn, $^*E_{red}$ is obtained by the equation $^*E_{red} = E_{red} + E_{00}$, where E_{00} stands for a potential corresponding to the excited state energy, taken as the highest-energy feature of the emission spectrum.[12]

[14] M. R. Wasielewski, *Chem. Rev.* **1992**, *92*, 435−461.

[15] J. N. Demas, G. A. Crosby, *J. Phys. Chem.* **1971**, *75*, 991−1008.

[16] K. Nakamaru, *Bull. Chem. Soc. Jpn.* **1982**, *55*, 2697−2705.

Received December 10, 1999
[I99452]